


Cubic Lower Record-Based Transmuted Family of Distributions: Theory, Estimation, Applications

Authors: CANER TANIŞ  
– Department of Statistics, Necmettin Erbakan University,
Türkiye
caner.tanis@erbakan.edu.tr

Received: Month 0000

Revised: Month 0000

Accepted: Month 0000

Abstract:

- In this study, a family of distributions called cubic lower record-based transmuted is provided. A special case of this family is proposed as an alternative exponential distribution. Several statistical properties are explored. We utilize nine different methods to estimate the parameters of the suggested distribution. In order to compare the performances of these methods, we consider a comprehensive Monte-Carlo simulation study. As a result of simulation study, we conclude that minimum absolute distance estimator is a valuable alternative to maximum likelihood estimator. Then, we carried out two real-world data examples to evaluate the fits of introduced distribution as well as its potential competitor ones. The findings of real-world data analysis show that the best-fitting distribution for both datasets is our model.

Keywords:

- *lower record values; transmuted distributions; point estimation; Monte Carlo simulation; real data analysis.*

AMS Subject Classification:

- 62E10, 62F10, 62P99.

1. INTRODUCTION

In last decades, the systematic proposition of lifetime distributions has become a key focus in the advancement of statistical modeling, especially by becoming flexibility and explicative power. Although classical distributions form the building blocks of probability theory, they often fall short when modeling real data sets exhibiting properties such as asymmetry, heavy tails, or multiple peaks. To overcome these limitations, interest has grown in transformation approaches and generalized distribution families. In this regard, the transmutation map introduced by [Shaw and Buckley \(2009\)](#) using a method based on order statistics is considered one of the most effective tools in the literature. The mathematical expression of the transmutation map defined in the relevant study ([Shaw and Buckley, 2009](#)) is given as follows:

Let X_1 and X_2 be independent and identically distributed (iid) random variables with cumulative distribution function (CDF) $G(\cdot)$ and probability density function (PDF) $g(\cdot)$, and $X_{1:n}$, $X_{2:n}$ be the first two order statistics associated with the sample.

Let us define random variable T

$$\begin{aligned} T &\stackrel{d}{=} X_{1:2}, \text{ with probability } \omega, \\ T &\stackrel{d}{=} X_{2:2}, \text{ with probability } 1 - \omega, \end{aligned}$$

and its corresponding CDF

$$\begin{aligned} F_T(x) &= \omega P(X_{1:2} \leq x) + (1 - \omega) P(X_{2:2} \leq x) \\ &= \omega \left\{ 1 - [1 - G(x)]^2 \right\} + (1 - \omega) [G(x)]^2 \\ (1.1) \quad &= 2\omega G(x) + (1 - 2\omega) [G(x)]^2, \end{aligned}$$

where $\omega \in (0, 1)$. Substituting $\omega = \frac{1+\lambda}{2}$ in Eq. (1.1), the CDF can be rewritten as follows:

$$(1.2) \quad F_T(x) = (1 + \lambda) G(x) - \lambda [G(x)]^2,$$

and its corresponding PDF

$$(1.3) \quad f_T(x) = (1 + \lambda) g(x) - 2\lambda G(x) g(x),$$

where $\lambda \in [-1, 1]$.

In last decades, the transmutation map based on the distributions of the order statistics has been used by many authors to generate the flexible statistical distributions. Some of these studies are listed as follows: [Aryal and Tsokos \(2011\)](#) proposed transmuted Weibull distribution as an alternative to Weibull distribution. [Mahmoud and Mandouh \(2013\)](#) studied on transmuted Fréchet distribution Transmuted inverse Rayleigh distribution is suggested by [Ahmad et al. \(2014\)](#). [Taniş et al. \(2020\)](#) provided transmuted complementary exponential power distribution. [Granzotto et al. \(2017\)](#) proposed the cubic rank transmuted family of distribution using the cubic rank transmutation map (CRTM) based on the distributions of first three order statistics. The CRTM can be summarized as follows:

Let X_1, X_2, X_3 be iid random variables with the CDF $G(x)$ and the PDF $g(x)$. Let $X_{1:n}, X_{2:n}$ and $X_{3:n}$ be the order statistics of this sample. Let us define a random variable Z

$$\begin{aligned} Z &\stackrel{d}{=} X_{1:3}, \text{ with probability } p_1, \\ Z &\stackrel{d}{=} X_{2:3}, \text{ with probability } p_2, \\ Z &\stackrel{d}{=} X_{3:3}, \text{ with probability } p_3, \end{aligned}$$

where $p_1 + p_2 + p_3 = 1$. The corresponding CDF of Z is

$$\begin{aligned} F_Z(x) &= p_1 P(X_{1:3} \leq x) + p_2 P(X_{2:3} \leq x) + p_3 P(X_{3:3} \leq x) \\ (1.4) \quad &= p_1 \{1 - [1 - G(x)]^3\} + 6p_2 \int_0^x \{G(t)[1 - G(t)]g(t)\} dt + p_3 [G(x)]^3 \\ &= 3p_1 G(x) + (3p_2 - 3p_1)[G(x)]^2 + (1 - 3p_2)[G(x)]^3. \end{aligned}$$

Substituting $3p_1 = \lambda_1$ and $3p_2 = \lambda_2$ into Eq. (1.4), the CDF and PDF of Z are obtained as

$$(1.5) \quad F_Z(x) = \lambda_1 G(x) + (\lambda_2 - \lambda_1)[G(x)]^2 + (1 - \lambda_2)[G(x)]^3,$$

and

$$(1.6) \quad f_Z(x) = g(x) \{ \lambda_1 + 2(\lambda_2 - \lambda_1)G(x) + 3(1 - \lambda_2)[G(x)]^2 \},$$

respectively, where $\lambda_1 \in [0, 1]$ and $\lambda_2 \in [-1, 1]$.

Granzotto et al. (2017) proposed two sub models of the cubic rank transmuted family of distributions (CRTFD) based on Weibull and log-logistic distributions. Saraçoğlu and Tanış (2018) introduced a new member of the CRTFD based on Kumaraswamy distribution. Also, the cubic rank transmuted Kumaraswamy distribution stands out as the first member of the CRTFD whose random variable is defined on the unit interval (0,1). Tanış and Saraçoğlu (2022a) studied on cubic rank transmuted inverse Rayleigh distribution. Tanış and Saraçoğlu (2023) introduced a new member of the CRTFD based on generalized Gompertz distribution. Likewise, the CRTFD as presented in Eq. (1.1), Balakrishnan and He (2021) suggested a new family of distributions based on the first two upper record statistics, namely record-based transmuted family of distributions (RBTFD). The RBTFD is obtained by record-based transmutation map (RBTM) defined as follows:

Let X_1 and X_2 be a random sample with two sizes from the distribution with CDF $G(\cdot)$ and PDF $g(\cdot)$, and $X_{U(1)}$ and $X_{U(2)}$ be upper records of the corresponding sample. Let us define a random variable R

$$\begin{aligned} R &\stackrel{d}{=} X_{U(1)}, \text{ with probability } p_1, \\ R &\stackrel{d}{=} X_{U(2)}, \text{ with probability } p_2, \end{aligned}$$

where $U_{(n)} = \min \{i : i > U(n-1), X_i > X_{U(n-1)}\}$ $\{U_{(n)}\}_{n=1}^{\infty}$ denotes upper record times and $\{X_{U(n)}\}_{n=1}^{\infty}$ refers to the corresponding record sequence (Balakrishnan and He, 2021; Arnold et al., 2008), $p_1 + p_2 = 1$ and R denotes a random variable from record-based transmuted distribution. Thus, the CDF of R is

$$\begin{aligned} F_R(x) &= p_1 P(X_{U(1)} \leq x) + p_2 P(X_{U(2)} \leq x) \\ (1.7) \quad &= G(x) + p \{ [1 - G(x)] \ln[1 - G(x)] \}, \end{aligned}$$

and its corresponding PDF

$$(1.8) \quad f_R(x) = g(x) \{1 + p[-\ln(1 - G(x)) - 1]\},$$

where $p \in (0, 1)$. Six sub-models of the RBTFD were introduced based on uniform, exponential, linear exponential, Weibull, Normal, logistic distributions in [Balakrishnan and He \(2021\)](#). However, no statistical inferences were provided regarding the proposed distributions in [Balakrishnan and He \(2021\)](#). [Taş and Saraçoğlu \(2022b\)](#) provided the statistical inferences and theoretical properties of the record-based transmuted Weibull and exponential distributions. In the literature, there are a few special cases of RBTFD based on Lindley [Taş \(2024\)](#), generalized linear exponential ([Arshad et al., 2024](#)), power Lomax ([Sakthivel and Nandhini, 2022](#)), Burr X ([Alrweili, 2025](#)), unit omega ([Pathak et al., 2024](#)), log-logistic ([Taş, 2025b](#)), and exponential power ([Taş, 2025a](#)). [Azhad et al. \(2023\)](#) provided a new record-based transmuted Kumaraswamy generalized family of distributions. Also, the cubic record-based transmuted family of distributions (CRBTFD), based on the distributions of the first three upper record values, was introduced by [Balakrishnan and He \(2021\)](#). The CRBTFD is derived using the cubic record-based transmutation map (CRBTM). The CRBTM is given as follows:

Let X_1, X_2 , and X_3 be iid random variables with the CDF $G(\cdot)$ and PDF $g(\cdot)$, and $X_{U(1)}, X_{U(2)}$, and $X_{U(3)}$ be upper records associated to the sample. Let us define a random variable R^*

$$\begin{aligned} R^* &\stackrel{d}{=} X_{U(1)}, \text{ with probability } p_1, \\ R^* &\stackrel{d}{=} X_{U(2)}, \text{ with probability } p_2, \\ R^* &\stackrel{d}{=} X_{U(3)}, \text{ with probability } 1 - p_1 - p_2, \end{aligned}$$

where R^* denotes a random variable from a distribution in CRBTFD and the CDF of R^* is

$$(1.9) \quad \begin{aligned} F_{R^*}(x) &= p_1 P(X_{U(1)} \leq x) + p_2 P(X_{U(2)} \leq x) + (1 - p_1 - p_2) P(X_{U(3)} \leq x) \\ &= 1 - [1 - G(x)] \{1 + (1 - p_1) [-\ln(1 - G(x))]\} \\ &\quad + [1 - G(x)] \left\{ \frac{1 - p_1 - p_2}{2} [-\ln(1 - G(x))]^2 \right\}, \end{aligned}$$

where $0 < p_1, p_2 < 1$ and $p_1 + p_2 \leq 1$. The corresponding PDF of R^* is

$$(1.10) \quad f_{R^*}(x) = g(x) \left\{ p_1 + p_2 [-\ln(1 - G(x))] + \frac{1 - p_1 - p_2}{2} [-\ln(1 - G(x))]^2 \right\}.$$

[Taş \(2026\)](#) provides statistical inferences about CRBTFD and a special case based on the Weibull distribution. In addition to RBTM, [Balakrishnan and He \(2021\)](#) suggested a dual record-based transmutation map (DRBTM) to generate flexible distributions from the dual record-based transmuted family of distributions (DRBTFD). The DRBTM is based on distributions of the first two lower record values and is defined as follows:

Let X_1 and X_2 be iid random variables with CDF $G(\cdot)$ and PDF $g(\cdot)$, and $X_{L(1)}$ and $X_{L(2)}$ be lower records of the corresponding sample. Let us define a random variable L

$$\begin{aligned} L &\stackrel{d}{=} X_{L(1)}, \text{ with probability } 1 - p, \\ L &\stackrel{d}{=} X_{L(2)}, \text{ with probability } p, \end{aligned}$$

where $L_{(n)} = \min \{i : i > L(n-1), X_i < X_{L(n-1)}\}$ $\{L_{(n)}\}_{n=1}^{\infty}$ refers to lower record times and $\{X_{L(n)}\}_{n=1}^{\infty}$ denotes its corresponding record sequence ([Balakrishnan and He, 2021](#);

(Arnold et al., 2008), L refers to a random variable distributed any member of DRBTFD. Thus, the CDF of L is

$$\begin{aligned}
 F_L(x) &= (1-p)P(X_{L(1)} \leq x) + pP(X_{L(2)} \leq x) \\
 &= (1-p)G(x) + p\{G(x)[1 - \ln(G(x))]\} \\
 (1.11) \qquad &= G(x)[1 - p \ln(G(x))],
 \end{aligned}$$

and its corresponding PDF

$$(1.12) \qquad f_L(x) = g(x) \{1 + p[-\ln(1 - G(x)) - 1]\}.$$

where $p \in (0, 1)$. In recent years, some studies about the DRBTFD were considered based on Fréchet (Tanış et al., 2021), power function (Tanış, 2021) and inverse Rayleigh (Tanış, 2022) distributions. Balakrishnan and He (2021) have briefly noted the order-3 version of the DRBTFD in their paper, though no detailed exposition was provided. Inspired by this work, the main objective of the present study is to propose the cubic lower record-based transmutation map (CLRBTM) and to provide a foundation for future studies aimed at generating new distributions within the cubic lower record-based transmuted family of distributions (CLRBTFD), using the distributions of first three lower record values.

The present work is organized as follows: In Section 2, we suggest the CLRBTM to generate continuous distribution. In addition, a special case of CLRBTFD based on exponential distribution is proposed in Section 2. Section 3 provides some distributional properties of the suggested distribution. In Section 4, we focus on the point estimation of the introduced distribution via nine different methods. Then, we design a comprehensive Monte Carlo (MC) simulation study to compare the performance of these estimators in Section 5. In Section 6, two real-life data examples are presented to illustrate the usefulness of the proposed distribution in real-life data modeling. Lastly, concluding remarks are given in Section 7.

2. CUBIC LOWER RECORD-BASED TRANSMUTED FAMILY OF DISTRIBUTIONS

Balakrishnan and He (2021) mentioned the CLRBTM based on distributions of the first three lower record values. However, no explicit formulation of CLRBTM was given in Balakrishnan and He (2021). In this section, we present both the construction of the CLRBTM and a detailed account of the resulting CLRBTFD obtained through the CLRBTM defined as follows:

Let $X_1, X_2,$ and X_3 be a random sample with CDF $G(\cdot)$ and PDF $g(\cdot)$, and $X_{L(1)}, X_{L(2)},$ and $X_{L(3)}$ be lower records of the same sample. Let us define a random variable L^*

$$\begin{aligned}
 L^* &\stackrel{d}{=} X_{L(1)}, \text{ with probability } p_1, \\
 L^* &\stackrel{d}{=} X_{L(2)}, \text{ with probability } p_2, \\
 L^* &\stackrel{d}{=} X_{L(3)}, \text{ with probability } 1 - p_1 - p_2,
 \end{aligned}$$

where $0 < p_1, p_2 < 1, p_1 + p_2 \leq 1$ and L^* denotes a random variable from a member of

CLRBTFD and the CDF of L^* is

$$\begin{aligned}
 F_{L^*}(x) &= p_1 P(X_{L(1)} \leq x) + p_2 P(X_{L(2)} \leq x) + (1 - p_1 - p_2) P(X_{L(3)} \leq x) \\
 &= p_1 G(x) + p_2 \{G(x) [1 - \ln(G(x))]\} \\
 &\quad + (1 - p_1 - p_2) \left\{ G(x) \left[1 - \ln(G(x)) + \frac{1}{2} (-\ln(G(x)))^2 \right] \right\} \\
 (2.1) \quad &= G(x) \left\{ 1 - (1 - p_1) \ln(G(x)) + \frac{1 - p_1 - p_2}{2} [-\ln(G(x))]^2 \right\}.
 \end{aligned}$$

Thus, its corresponding PDF of L^* is

$$(2.2) \quad f_{L^*}(x) = g(x) \left\{ p_1 - p_2 \ln(G(x)) + \frac{1 - p_1 - p_2}{2} [\ln(G(x))]^2 \right\}.$$

2.1. Cubic lower record-based transmuted exponential distribution

In this section, we propose the cubic lower record-based transmuted exponential distribution (CLRBTE) using the CLRBTM.

Let $X \sim \text{CLRBTE}(\lambda, p_1, p_2)$ denote a random variable. By substituting the exponential CDF $G(x) = 1 - e^{-\lambda x}$ into Eq. (2.1), the CDF and PDF of X are obtained as follows:

$$(2.3) \quad F_{\text{CLRBTE}}(x) = \left(1 - e^{-\lambda x}\right) \left\{ 1 - (1 - p_1) \left[\ln\left(1 - e^{-\lambda x}\right) \right] + \frac{1 - p_1 - p_2}{2} \left[\ln\left(1 - e^{-\lambda x}\right) \right]^2 \right\},$$

and

$$(2.4) \quad f_{\text{CLRBTE}}(x) = \lambda e^{-\lambda x} \left\{ p_1 - p_2 \left[\ln\left(1 - e^{-\lambda x}\right) \right] + \frac{1 - p_1 - p_2}{2} \left[\ln\left(1 - e^{-\lambda x}\right) \right]^2 \right\},$$

respectively, where $x > 0$, $p_1, p_2 \in [0, 1]$ and $p_1 + p_2 \leq 1$. The CLRBTE distribution reduces to the standard exponential distribution when $p_1 = 1$ and $p_2 = 0$.

2.1.1. Density shape

In this section, we explore the shape of the PDF via Theorem 2.1.

Theorem 2.1. *The PDF of the CLRBTE distribution in Eq. (2.4) is strictly decreasing for all $x \geq 0$ whenever either of the following criteria is fulfilled:*

- $p_1 + p_2 = 1$ and $p_2 \geq 0$.
- $\lambda > 0$, $p_1 = 1$, and $p_2 = 0$.

Proof: Let us define the transformation $u = u(x) = 1 - e^{-\lambda x}$ such that $u \in (0, 1)$ and its derivative is $\frac{du}{dx} = \lambda(1 - u)$ to assess the monotonicity of the PDF.

Hence, the PDF of the CLRBTE distribution can be rewritten as follows:

$$(2.5) \quad f(x) = \lambda(1-u)K(u),$$

where $K(u) = p_1 - p_2 \ln(u) + \eta[\ln(u)]^2$ and $\eta = \frac{1-p_1-p_2}{2}$. The monotonicity of PDF can be determined by the sign of the derivative of its logarithm, which we denote as $\psi(x)$:

$$(2.6) \quad \psi(x) = \frac{d}{dx} \ln f(x) = \frac{f'(x)}{f(x)} = \lambda(1-u) \left[\frac{K'(u)}{K(u)} - \frac{1}{1-u} \right].$$

By substituting the derivative of the $K'(u) = \frac{1}{u} [-p_2 + 2\eta \ln(u)]$ in Eq. (2.6), we obtain the explicit form of the monotonicity function:

$$(2.7) \quad \psi(x) = \lambda(1-u) \left[\frac{-p_2 + 2\eta \ln(u)}{uK(u)} - \frac{1}{1-u} \right].$$

Under the first condition ($p_1 + p_2 = 1$), the parameter η becomes zero, which simplifies $K'(u) = -p_2/u$. Provided that $p_2 \geq 0$, $u > 0$, and $K(u) > 0$, the term $\psi(x)$ remains strictly negative for all $x > 0$. This confirms that $f(x)$ is strictly decreasing. Under the second condition ($p_1 = 1, p_2 = 0$), the expression reduces to the exponential distribution where $\psi(x) = -\lambda < 0$. In either case, the negative sign of $\psi(x)$ implies a strictly decreasing PDF. Thus, the proof is completed. \square

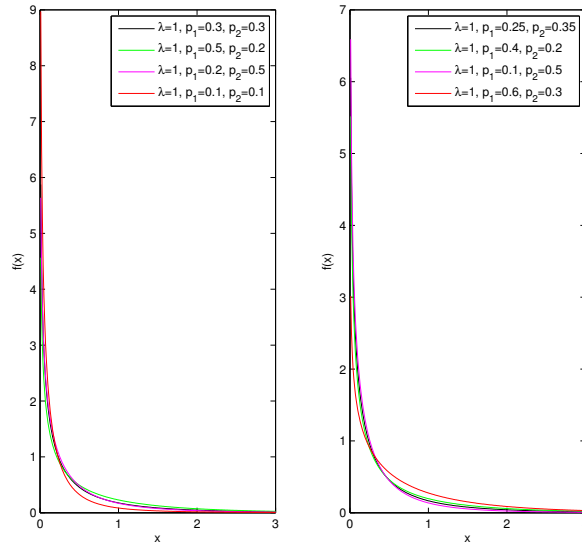


Figure 1: The PDFs of CLRBTE distribution under the different values of parameters

Figure 1 illustrates the possible PDF shapes associated with the CLRBTE distribution in the parameters selected values. From Figure 1, we clearly see that the CLRBTE distribution has a decreasing PDF.

3. SOME DISTRIBUTIONAL PROPERTIES

This section explores some statistical properties of the CLRBTE distribution, namely, hazard function (HF), moments, mean, variance, coefficient of variation, coefficient of skew-

ness, and coefficient of kurtosis.

3.1. Hazard function

The HF of the CLRBTE distribution is

$$h(x) = \frac{f(x)}{1 - F(x)} = \frac{\lambda e^{-\lambda x} \left\{ p_1 - p_2 [\ln(1 - e^{-\lambda x})] + \frac{1-p_1-p_2}{2} [\ln(1 - e^{-\lambda x})]^2 \right\}}{1 - (1 - e^{-\lambda x}) \left\{ 1 - (1 - p_1) [\ln(1 - e^{-\lambda x})] + \frac{1-p_1-p_2}{2} [\ln(1 - e^{-\lambda x})]^2 \right\}},$$

where $F(\cdot)$ and $f(\cdot)$ are the CDF and PDF of CLRBTE distribution respectively given in Eqs. (2.3) and (2.4) Figure 2 illustrates the possible hazard shapes of the CLRBTE distribution. Figure 2 displays that the hf is decreasing shape.

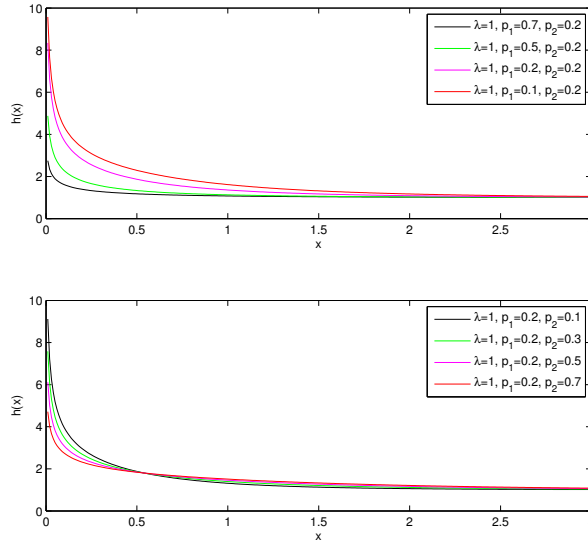


Figure 2: The HF shapes of the CLRBTE distribution in the different values of parameters

3.2. Moments

In this subsection, we present the r -th central moment for the $CLRBTE(\lambda, p_1, p_2)$ distribution via the Theorem 3.1.

Theorem 3.1. *Let X be a random variable from the $CLRBTE(\lambda, p_1, p_2)$ distribution. The r -th central moment is*

$$(3.1) \quad \mu'_r = \frac{\Gamma(r+1)}{\lambda^r} \left[p_1 + p_2 \sum_{j=1}^{\infty} \frac{1}{j} \left(1 - \frac{1}{(j+1)^r} \right) + \frac{1-p_1-p_2}{2} \sum_{j=1}^{\infty} \frac{H_j}{(j+1)^{r+1}} \right],$$

where $\Gamma(\cdot)$ is the gamma function and $H_j = \sum_{k=1}^j \frac{1}{k}$ denotes the j -th harmonic number.

Proof: The r -th raw moment is defined by the integral:

$$(3.2) \quad \mu'_r = \int_0^\infty x^r \lambda e^{-\lambda x} \left[p_1 - p_2 \ln(1 - e^{-\lambda x}) + \frac{p_3}{2} (\ln(1 - e^{-\lambda x}))^2 \right] dx.$$

Let $u = 1 - e^{-\lambda x}$ be a transformation. Then, $e^{-\lambda x} = 1 - u$, $x = -\frac{1}{\lambda} \ln(1 - u)$, and $du = \lambda e^{-\lambda x} dx$. The limits of integration change from $[0, \infty)$ to $[0, 1)$. Substituting these into the integral:

$$(3.3) \quad \mu'_r = \frac{1}{\lambda^r} \int_0^1 [-\ln(1 - u)]^r \left[p_1 - p_2 \ln u + \frac{p_3}{2} (\ln u)^2 \right] du.$$

Expanding the integral into three parts:

$$(3.4) \quad \mu'_r = \frac{1}{\lambda^r} \left[p_1 I_1 - p_2 I_2 + \frac{p_3}{2} I_3 \right],$$

where: $I_1 = \int_0^1 [-\ln(1 - u)]^r du = \Gamma(r + 1)$, $I_2 = \int_0^1 [-\ln(1 - u)]^r \ln u du$, $I_3 = \int_0^1 [-\ln(1 - u)]^r (\ln u)^2 du$. Then, we use the power series expansion $\ln(1 - u) = -\sum_{j=1}^\infty \frac{u^j}{j}$ to assess I_2 and I_3 . In order to derive the form of the series more directly, let us consider the following identity involving the integral of logarithmic functions:

$$(3.5) \quad I_1 = \int_0^1 u^j (-\ln u)^r du = \frac{\Gamma(r + 1)}{(j + 1)^{r+1}}.$$

The integrals I_2 and I_3 are transformed into infinite series by expanding the term $[-\ln(1 - u)]^r$ and applying the summation properties of the harmonic numbers H_j . More explicitly, the integral of the logarithmic terms:

$$(3.6) \quad I_2 = -\Gamma(r + 1) \sum_{j=1}^\infty \frac{1}{j} \left(1 - \frac{1}{(j + 1)^r} \right),$$

and for the squared logarithmic term I_3 :

$$(3.7) \quad I_3 = \Gamma(r + 1) \sum_{j=1}^\infty \frac{H_j}{(j + 1)^{r+1}}.$$

By substituting the integral identities for I_1, I_2 , and I_3 given in Eqs. (3.5), (3.6) and (3.7) into the expanded expression of the raw moment in Eq. (3.4) and factoring out the common term $\frac{\Gamma(r+1)}{\lambda^r}$, the final analytical representation of the r -th raw moment is derived as follows:

$$\mu'_r = \frac{\Gamma(r + 1)}{\lambda^r} \left[p_1 + p_2 \sum_{j=1}^\infty \frac{1}{j} \left(1 - \frac{1}{(j + 1)^r} \right) + \frac{1 - p_1 - p_2}{2} \sum_{j=1}^\infty \frac{H_j}{(j + 1)^{r+1}} \right].$$

Thus, the proof is completed. □

Then, we substitute $r = 1, 2, 3$, and 4 in Eq. (3.1), the first four raw moments of the CLRBTE distribution are explicitly obtained. Let $p_3 = 1 - p_1 - p_2$; then the analytical forms of these moments are presented as follows:

The mean of the distribution ($r = 1$) is given by

$$(3.8) \quad \mu'_1 = \frac{1}{\lambda} \left[p_1 + p_2 (1 - \ln 2) + \frac{p_3}{2} \left(2 - \frac{\pi^2}{6} \right) \right],$$

the second raw moment ($r = 2$) is

$$(3.9) \quad \mu'_2 = \frac{2}{\lambda^2} \left[p_1 + p_2 \left(1 - \frac{\pi^2}{12} \right) + \frac{p_3}{2} \left(\zeta(3) - \frac{\pi^2}{12} + 1 \right) \right],$$

the third raw moment ($r = 3$) is obtained as

$$(3.10) \quad \mu'_3 = \frac{6}{\lambda^3} \left[p_1 + p_2 \left(1 - \frac{3}{4}\zeta(3) \right) + \frac{p_3}{2} \left(\frac{\pi^4}{72} - \frac{3}{4}\zeta(3) + 1 \right) \right],$$

and the fourth raw moment ($r = 4$) is expressed as

$$(3.11) \quad \mu'_4 = \frac{24}{\lambda^4} \left[p_1 + p_2 \left(1 - \frac{7\pi^4}{720} \right) + \frac{p_3}{2} \left(\zeta(5) - \frac{7\pi^4}{720} + 1 \right) \right],$$

where $\zeta(s)$ denotes the Riemann Zeta function defined by $\zeta(s) = \sum_{n=1}^{\infty} n^{-s}$ for $s > 1$. The numerical convergence of these series-based expressions has been verified against direct numerical integration, ensuring the mathematical consistency of the derived moments across a wide range of parameter values.

3.3. Coefficients of variation, skewness and kurtosis

In this subsection, we introduce the Coefficient of skewness γ_1 and coefficient of kurtosis γ_2 regarding CLRBTE (λ, p_1, p_2) distribution are given in Eqs. (3.12) and (3.13).

$$(3.12) \quad \gamma_1 = \frac{\mu'_3 - 3\mu'_2\mu'_1 + 2(\mu'_1)^3}{\sigma^3},$$

and

$$(3.13) \quad \gamma_2 = \frac{\mu'_4 - 4\mu'_3\mu'_1 + 6\mu'_2(\mu'_1)^2 - 3(\mu'_1)^4}{\sigma^4},$$

respectively, where σ^2 is variance, $\sigma^2 = \mu'_2 - (\mu'_1)^2$. Also, the variation coefficient is

$$(3.14) \quad \text{CV} = \frac{\sigma}{\mu'_1}.$$

Table 1: Some descriptive statistics in various values of parameters

λ	p_1	p_2	μ'_1	σ^2	σ	CV	γ_1	γ_2
0.5	0.5	0.3	1.2551	3.9544	1.9886	1.5844	1.9733	7.8140
1.0	0.5	0.3	0.6276	0.9886	0.9943	1.5844	1.9733	7.8140
2.0	0.5	0.3	0.3138	0.2472	0.4971	1.5844	1.9733	7.8140
1.5	0.1	0.6	0.2249	0.3169	0.5630	2.5030	2.4919	8.9703
1.5	0.2	0.6	0.2797	0.3168	0.5629	2.0121	2.4156	9.7480
1.5	0.3	0.6	0.3346	0.3107	0.5574	1.6661	2.4135	10.8809
0.7	0.4	0.1	0.7421	2.5622	1.6007	2.1570	1.8052	5.6367
0.7	0.4	0.2	0.7605	2.3253	1.5249	2.0050	1.8821	6.3108
0.7	0.4	0.5	0.8160	1.6107	1.2691	1.5554	2.2706	10.0412

Table 1 provides the descriptive statistics of the CLRBTE distribution for selected combinations of the parameters λ , p_1 , and p_2 . As the scale parameter λ increases, the values of μ'_1 , σ^2 , and σ decrease, while CV , γ_1 , and γ_2 remain constant. This confirms that λ affects only the scale of the distribution. When p_1 increases (with λ and p_2 fixed), μ'_1 and γ_2 increase, whereas CV and γ_1 decrease. Also, there is an increase in p_2 leads to an increase in μ'_1 , γ_1 , and γ_2 , however causes a decrease in σ^2 and σ . In all cases, $\gamma_1 > 0$ and $\gamma_2 > 3$ indicate that the CLRBTE distribution is right-skewed and leptokurtic, demonstrating its flexibility for modeling various data structures.

4. POINT ESTIMATION

In this section, we tackle the point estimation of the CLRBTE distribution. Nine methods are utilized to estimate the parameters λ , p_1 , and p_2 .

4.1. Maximum likelihood estimator

This subsection explores ML estimators (MLEs) of the parameters λ , p_1 , and p_2 . Let X_1, X_2, \dots, X_n be an iid random variables from the CLRBTE and x_1, x_2, \dots, x_n denote the observed values of the sample. Then, the log-likelihood function is as follows:

$$(4.1) \quad \begin{aligned} \ell(x; \lambda, p_1, p_2) &= n \ln(\lambda) - \lambda \sum_{i=1}^n x_i \\ &+ \sum_{i=1}^n \ln \left\{ p_1 - p_2 \left[\ln(1 - e^{-\lambda x_i}) \right] + \frac{1 - p_1 - p_2}{2} \left[\ln(1 - e^{-\lambda x_i}) \right]^2 \right\}. \end{aligned}$$

The first-order partial derivatives of $\ell(x; \lambda, p_1, p_2)$ over the parameters λ , p_1 , and p_2 are given by

$$(4.2) \quad \begin{aligned} \frac{\partial \ell(x; \lambda, p_1, p_2)}{\partial \lambda} &= \frac{n}{\lambda} - \sum_{i=1}^n x_i \\ &+ \sum_{i=1}^n \frac{x_i e^{-\lambda x_i} \left\{ -p_2 + (1 - p_1 - p_2) \left[\ln(1 - e^{-\lambda x_i}) \right] \right\}}{(1 - e^{-\lambda x_i}) \left\{ p_1 - p_2 \left[\ln(1 - e^{-\lambda x_i}) \right] + \frac{1 - p_1 - p_2}{2} \left[\ln(1 - e^{-\lambda x_i}) \right]^2 \right\}}, \end{aligned}$$

$$(4.3) \quad \frac{\partial \ell(x; \lambda, p_1, p_2)}{\partial p_1} = \sum_{i=1}^n \frac{1 - \frac{1}{2} \left[\ln(1 - e^{-\lambda x_i}) \right]^2}{p_1 - p_2 \left[\ln(1 - e^{-\lambda x_i}) \right] + \frac{1 - p_1 - p_2}{2} \left[\ln(1 - e^{-\lambda x_i}) \right]^2},$$

$$(4.4) \quad \frac{\partial \ell(x; \lambda, p_1, p_2)}{\partial p_2} = \sum_{i=1}^n \frac{-\ln(1 - e^{-\lambda x_i}) - \frac{1}{2} \left[\ln(1 - e^{-\lambda x_i}) \right]^2}{p_1 - p_2 \left[\ln(1 - e^{-\lambda x_i}) \right] + \frac{1 - p_1 - p_2}{2} \left[\ln(1 - e^{-\lambda x_i}) \right]^2},$$

respectively. The MLEs of the parameters λ , p_1 , and p_2 are values of parameters that maximize $\ell(x; \lambda, p_1, p_2)$. The MLEs are simultaneously solution the Equations obtained by setting each of the Eqs. (4.2), (4.3), and (4.4) equal to zero. Some numerical methods, namely, Newton-Raphson and Nelder Mead can be utilized to solve this optimization problem

4.2. Least squares estimator

In this subsection, we examine the LS estimators (LSEs) the parameters λ , p_1 , and p_2 . The LSE is proposed by Swain et al. (1988) as an alternative to the MLE. The LSEs can be obtained by minimizing the function given in Eq. (4.5).

$$(4.5) \quad LS(x_i) = \sum_{i=1}^n \left[F(x_{i:n}) - \frac{i}{n+1} \right]^2,$$

where $x_{i:n}$ for $i = 1, 2, \dots, n$ denote the order statistics.

4.3. Weighted least squares estimator

This subsection introduces the WLS estimators (WLSEs) of parameters λ , p_1 , and p_2 for the CLRBTE via the method proposed by Swain et al. (1988). We derive the WLSEs by minimizing the Eq. (4.6).

$$(4.6) \quad WLS(x_i) = \sum_{i=1}^n \frac{(n+1)^2(n+2)}{i(n-i+1)} \left[F(x_{i:n}) - \frac{i}{n+1} \right]^2.$$

4.4. Anderson-Darling estimator

This subsection discusses the AD estimators (ADEs) of parameters λ , p_1 , and p_2 . The ADEs of the parameters λ , p_1 , and p_2 can be derived by minimizing Eq (4.7).

$$(4.7) \quad AD(x_i) = -n - \frac{1}{n} \sum_{i=1}^n (2i-1) [\ln F(x_{i:n}) + \ln(1 - F(x_{n-i-1:n}))].$$

4.5. Cramér-von Mises estimator

In this subsection, we study the CvM estimators (CvMEs) of the parameters λ , p_1 , and p_2 . The Cramér-von Mises method is suggested by Choi and Bulgren (1968). We compute the CvMEs by maximizing the function in Eq. (4.8).

$$(4.8) \quad C(x_i) = \frac{1}{12n} + \sum_{i=1}^n \left[F(x_{i:n}) - \frac{2i-1}{2n} \right]^2.$$

4.6. Maximum product of spacings estimator

This subsection introduces the MPS method proposed by [Cheng and Amin \(1983\)](#) and [Ranneby \(1984\)](#) as an alternative to the ML method, the MPS method based on maximizing the function in Eq. (4.9) to obtain the MPS estimators (MPSEs).

$$(4.9) \quad \delta(x_i) = \frac{1}{n+1} \sum_{i=1}^{n+1} \ln I_i(x_i),$$

where $I_i(x_i) = F(x_{i:n}) - F(x_{i-1:n})$, $F(x_{0:n}) = 0$ and $F(x_{n+1:n}) = 1$.

4.7. Right tail Anderson Darling estimator

In this subsection, we explore the RTAD estimators (RTADEs) of parameters λ , p_1 , and p_2 . We derive the RTADEs by minimizing the Eq. (4.10).

$$(4.10) \quad L(\lambda, p_1, p_2) = \frac{n}{2} - 2 \sum_{i=1}^n F(x_{i:n}) - \frac{1}{n} \sum_{i=1}^n (2i-1) \ln(1 - F(x_{n-i+1})).$$

4.8. Minimum spacing absolute distance estimator

In this subsection, we suggest the MSAD estimators (MSADEs) of the parameters λ , p_1 , and p_2 . The MSADEs of parameters λ , p_1 , and p_2 are computed by minimizing the function given in Eq. (4.11).

$$(4.11) \quad \Lambda(\lambda, p_1, p_2 | x_i) = \sum_{i=1}^{n+1} \left| I_i - \frac{1}{n+1} \right|.$$

4.9. Minimum spacing absolute-log distance estimator

In this subsection, we tackle the MSALD estimators (MSALDEs) of parameters λ , p_1 , and p_2 . [Torabi \(2008\)](#) suggested the MSALD method as an alternative the ML. We derive the MSALDEs of the parameters λ , p_1 , and p_2 by minimizing the Eq. (4.12)

$$(4.12) \quad \Psi(\lambda, p_1, p_2 | x_i) = \sum_{i=1}^{n+1} \left| I_i - \ln \left(\frac{1}{n+1} \right) \right|.$$

5. SIMULATION

This section provides an extensive MC simulation study to evaluate the performance of the mentioned estimators given in Section 4. In MC simulation study, we carry out the following settings:

- The sample sizes; $n = 50, 100, 200, 500, 1000$
- The number of repetition: 5000
- Initial values of parameters λ , p_1 and p_2 are taken as follows:
Senerio_I = $(\lambda = 1.5, p_1 = 0.5, p_2 = 0.3)$,
Senerio_{II} = $(\lambda = 0.5, p_1 = 0.4, p_2 = 0.5)$,
Senerio_{III} = $(\lambda = 0.6, p_1 = 0.3, p_2 = 0.2)$,
Senerio_{IV} = $(\lambda = 2, p_1 = 0.2, p_2 = 0.4)$.

We utilize bias, mean squared error (MSE), and mean relative error (MRE) in order to evaluate the performance of the examined estimators. These measures are given by

$$Bias = \frac{1}{5000} \sum_{i=1}^{5000} (\hat{Y} - \Upsilon), MSE = \frac{1}{5000} \sum_{i=1}^{5000} (\hat{Y} - \Upsilon)^2, MRE = \frac{1}{5000} \sum_{i=1}^{5000} \frac{|\hat{Y} - \Upsilon|}{|\Upsilon|},$$

where $\Upsilon = (\lambda, p_1, p_2)$.

5.1. Random sample generation

To generate random samples from the $CLRBTE(\lambda, p_1, p_2)$ distribution, we use an acceptance-rejection (AR) sampling algorithm. We choose the Weibull distribution as the proposal distribution in the AR algorithm. The AR algorithm is given as follows:

Algorithm 1.

A1. Generate data on random variable $Y \sim Weibull(\gamma, \nu)$ with the PDF g given as follows:

$$g(\gamma, \nu) = \gamma \nu x^{\nu-1} e^{-\gamma x^\nu}.$$

A2. Generate U from standard uniform distribution(independent of Y).

A3. If

$$U < \frac{f(Y; \lambda, p_1, p_2)}{k \times g(Y; \gamma, \nu)},$$

then set $X = Y$ (“accept”); otherwise go back to A1 (“reject”), where the PDF $f(\cdot)$ is given as in Eq. (2.4) and

$$k = \max_{z \in \mathbb{R}_+} \frac{f(z; \lambda, p_1, p_2)}{g(z; \gamma, \nu)}.$$

In MC simulation study, We use Algorithm 1 to generate random sample. Furthermore, all optimization problems are solved via R software (R Core Team, 2024) and `optim()` function, with the BFGS (Broyden–Fletcher–Goldfarb–Shanno) (Nocedal and Wright, 2006) algorithm.

We report the findings of MC simulation study in Tables 2-5.

Table 2: The simulation results in $\lambda = 1.5$, $p_1 = 0.5$ and $p_2 = 0.3$

Estimator	n	Bias			MSE			MRE		
		$\hat{\lambda}$	\hat{p}_1	\hat{p}_2	$\hat{\lambda}$	\hat{p}_1	\hat{p}_2	$\hat{\lambda}$	\hat{p}_1	\hat{p}_2
MLE	50	-0.0817	-0.0702	0.0669	0.1155	0.0267	0.0327	0.1793	0.2541	0.4837
	100	-0.0773	-0.0619	0.0567	0.0946	0.0251	0.0318	0.1675	0.2503	0.4736
	200	-0.0542	-0.0387	0.0454	0.0791	0.0199	0.0290	0.1468	0.2168	0.4673
	500	-0.0165	-0.0368	0.0377	0.0521	0.0174	0.0268	0.1158	0.2115	0.4287
	1000	0.0054	-0.0109	0.0068	0.0240	0.0090	0.0140	0.0782	0.1429	0.3122
LSE	50	-0.3657	-0.1937	0.0991	0.2744	0.0624	0.0485	0.3053	0.4519	0.6268
	100	-0.2759	-0.1618	0.0811	0.2008	0.0557	0.0434	0.2593	0.4226	0.5871
	200	-0.1748	-0.1070	0.0780	0.1299	0.0401	0.0427	0.2040	0.3398	0.5790
	500	-0.0970	-0.0579	0.0437	0.0807	0.0273	0.0334	0.1579	0.2717	0.5083
	1000	-0.0357	-0.0200	0.0082	0.0475	0.0160	0.0219	0.1159	0.2015	0.3982
WLSE	50	-0.3604	-0.1953	0.1177	0.2353	0.0609	0.0448	0.2806	0.4346	0.5916
	100	-0.2718	-0.1625	0.1107	0.1761	0.0523	0.0402	0.2406	0.3957	0.5657
	200	-0.1767	-0.1088	0.0867	0.1174	0.0382	0.0399	0.1867	0.3145	0.5457
	500	-0.0755	-0.0475	0.0422	0.0570	0.0205	0.0271	0.1280	0.2272	0.4434
	1000	-0.0236	-0.0135	0.0067	0.0292	0.0106	0.0162	0.0887	0.1594	0.3350
ADE	50	-0.2347	-0.1546	0.1243	0.1724	0.0467	0.0447	0.2366	0.3716	0.5845
	100	-0.2265	-0.1477	0.1231	0.1491	0.0459	0.0416	0.2203	0.3703	0.5675
	200	-0.1563	-0.1020	0.0901	0.1029	0.0351	0.0388	0.1773	0.3025	0.5340
	500	-0.0753	-0.0487	0.0455	0.0562	0.0204	0.0270	0.1273	0.2267	0.4432
	1000	-0.0243	-0.0146	0.0087	0.0294	0.0107	0.0161	0.0885	0.1591	0.3335
CvME	50	-0.2392	-0.1707	0.1427	0.1982	0.0523	0.0556	0.2525	0.4169	0.6639
	100	-0.2114	-0.1487	0.1259	0.1660	0.0504	0.0538	0.2338	0.4032	0.6578
	200	-0.1445	-0.1003	0.0883	0.1169	0.0377	0.0449	0.1936	0.3303	0.5870
	500	-0.0853	-0.0552	0.0469	0.0769	0.0263	0.0334	0.1545	0.2677	0.5078
	1000	-0.0303	-0.0188	0.0098	0.0462	0.0157	0.0219	0.1149	0.2000	0.3972
MPSE	50	-0.3487	-0.1682	0.0817	0.2479	0.0584	0.0382	0.2803	0.3977	0.5275
	100	-0.3225	-0.1594	0.0741	0.2184	0.0534	0.0348	0.2621	0.3797	0.5038
	200	-0.2534	-0.1390	0.0679	0.1704	0.0534	0.0343	0.2173	0.3608	0.4852
	500	-0.1553	-0.0893	0.0270	0.1017	0.0371	0.0267	0.1559	0.2807	0.4469
	1000	-0.0704	-0.0385	0.0198	0.0435	0.0159	0.0178	0.0961	0.1740	0.3449
TADE	50	-0.2227	-0.1321	0.0761	0.1725	0.0457	0.0410	0.2334	0.3567	0.5501
	100	-0.2175	-0.1238	0.0661	0.1577	0.0422	0.0403	0.2234	0.3424	0.5480
	200	-0.1572	-0.0953	0.0491	0.1087	0.0366	0.0367	0.1794	0.3069	0.5224
	500	-0.0765	-0.0461	0.0349	0.0585	0.0221	0.0308	0.1268	0.2337	0.4756
	1000	-0.0292	-0.0170	0.0104	0.0294	0.0113	0.0183	0.0876	0.1618	0.3518
MSADE	50	-0.2380	-0.1109	0.0482	0.1518	0.0349	0.0320	0.2077	0.2979	0.4817
	100	-0.2223	-0.1037	0.0361	0.1447	0.0307	0.0289	0.2028	0.2843	0.4564
	200	-0.1595	-0.0852	0.0283	0.0983	0.0304	0.0287	0.1610	0.2689	0.4559
	500	-0.0829	-0.0500	0.0161	0.0599	0.0213	0.0276	0.1235	0.2211	0.4428
	1000	-0.0433	-0.0244	0.0047	0.0351	0.0132	0.0202	0.0937	0.1706	0.3725
MSALDE	50	-0.2909	-0.1551	0.0713	0.2344	0.0577	0.0430	0.2674	0.3980	0.5649
	100	-0.2840	-0.1488	0.0674	0.2122	0.0526	0.0415	0.2556	0.3836	0.5440
	200	-0.2184	-0.1224	0.0581	0.1580	0.0513	0.0388	0.2120	0.3589	0.5224
	500	-0.1339	-0.0783	0.0392	0.0980	0.0353	0.0359	0.1578	0.2812	0.5185
	1000	-0.0650	-0.0373	0.0254	0.0474	0.0177	0.0221	0.1039	0.1907	0.3868

Table 3: The simulation results in $\lambda = 0.5$, $p_1 = 0.4$ and $p_2 = 0.5$

Estimator	n	Bias			MSE			MRE		
		$\hat{\lambda}$	\hat{p}_1	\hat{p}_2	$\hat{\lambda}$	\hat{p}_1	\hat{p}_2	$\hat{\lambda}$	\hat{p}_1	\hat{p}_2
MLE	50	0.0767	0.0598	-0.0517	0.0519	0.0459	0.0778	0.3493	0.4384	0.4778
	100	0.0456	0.0371	-0.0505	0.0307	0.0413	0.0733	0.2731	0.4272	0.4621
	200	0.0235	0.0317	-0.0340	0.0205	0.0389	0.0672	0.2241	0.3982	0.4372
	500	0.0149	0.0205	-0.0332	0.0139	0.0355	0.0545	0.1908	0.3942	0.3887
	1000	0.0024	0.0061	-0.0282	0.0081	0.0245	0.0354	0.1426	0.3155	0.3072
LSE	50	0.0218	0.0605	-0.3040	0.0731	0.1186	0.4328	0.4138	0.6430	1.0035
	100	0.0213	0.0410	-0.1742	0.0522	0.0848	0.2185	0.3389	0.5571	0.7228
	200	0.0177	0.0383	-0.1158	0.0316	0.0702	0.1491	0.2742	0.5394	0.6079
	500	0.0136	0.0322	-0.0845	0.0202	0.0484	0.0871	0.2200	0.4608	0.4771
	1000	0.0030	0.0257	-0.0601	0.0109	0.0314	0.0518	0.1738	0.3801	0.3739
WLSE	50	-0.0593	-0.0619	-0.2289	0.0554	0.0910	0.4196	0.3751	0.5881	0.9259
	100	-0.0438	-0.0357	-0.0368	0.0319	0.0621	0.1445	0.2847	0.5139	0.6127
	200	-0.0231	-0.0228	-0.0131	0.0230	0.0589	0.1014	0.2438	0.5134	0.5244
	500	-0.0126	-0.0221	-0.0220	0.0155	0.0436	0.0662	0.2017	0.4424	0.4313
	1000	0.0034	0.0093	-0.0352	0.0082	0.0250	0.0398	0.1501	0.3350	0.3312
ADE	50	-0.0144	-0.0108	-0.1276	0.0460	0.0837	0.2516	0.3388	0.5766	0.7054
	100	0.0086	0.0103	-0.0510	0.0332	0.0539	0.1112	0.2831	0.4779	0.5378
	200	0.0017	-0.0068	-0.0451	0.0222	0.0526	0.0904	0.2362	0.4909	0.4975
	500	0.0004	0.0057	-0.0465	0.0144	0.0382	0.0633	0.1936	0.4183	0.4200
	1000	0.0003	0.0017	-0.0306	0.0080	0.0252	0.0392	0.1491	0.3357	0.3292
CvME	50	0.0909	0.0939	-0.1706	0.0810	0.1318	0.3346	0.4138	0.6573	0.8770
	100	0.0609	0.0588	-0.1165	0.0538	0.0876	0.1916	0.3334	0.5486	0.6765
	200	0.0458	0.0600	-0.1042	0.0330	0.0703	0.1422	0.2730	0.5275	0.5949
	500	0.0340	0.0418	-0.0792	0.0203	0.0475	0.0853	0.2169	0.4512	0.4725
	1000	0.0191	0.0308	-0.0597	0.0108	0.0308	0.0509	0.1715	0.3742	0.3704
MPSE	50	-0.1279	-0.0713	-0.6228	0.0693	0.1855	1.9005	0.4440	0.6591	1.4353
	100	-0.0941	-0.0790	-0.1894	0.0451	0.0530	0.2454	0.3498	0.5196	0.6977
	200	-0.0752	-0.0608	-0.0619	0.0318	0.0546	0.0978	0.2935	0.4965	0.4990
	500	-0.0511	-0.0549	-0.0328	0.0207	0.0473	0.0638	0.2358	0.4727	0.4138
	1000	-0.0397	0.0448	0.0109	0.0123	0.0358	0.0386	0.1783	0.3896	0.3290
TADE	50	-0.0253	-0.0232	-0.2083	0.0572	0.0997	0.3458	0.3764	0.6191	0.8542
	100	-0.0257	-0.0142	-0.1014	0.0349	0.0674	0.1475	0.2963	0.5384	0.6186
	200	-0.0136	-0.0085	-0.0495	0.0232	0.0535	0.1045	0.2443	0.4992	0.5281
	500	-0.0083	-0.0028	-0.0473	0.0149	0.0418	0.0710	0.1998	0.4373	0.4344
	1000	-0.0053	0.0006	-0.0298	0.0085	0.0264	0.0423	0.1513	0.3414	0.3373
MSADE	50	-0.0638	-0.0235	-0.2072	0.0427	0.0427	0.1803	0.3405	0.3807	0.5908
	100	-0.0389	-0.0203	-0.1011	0.0281	0.0313	0.0959	0.2736	0.3782	0.4394
	200	-0.0288	-0.0110	-0.0814	0.0217	0.0392	0.0755	0.2367	0.3395	0.3937
	500	-0.0173	-0.0103	-0.0527	0.0146	0.0305	0.0508	0.1922	0.3375	0.3337
	1000	-0.0137	-0.0084	-0.0296	0.0087	0.0236	0.0354	0.1466	0.2974	0.2850
MSALDE	50	-0.0876	-0.0546	-0.3317	0.0638	0.0740	0.3293	0.4247	0.5390	0.8593
	100	-0.0740	-0.0535	-0.1621	0.0422	0.0596	0.1872	0.3373	0.5314	0.6540
	200	-0.0589	-0.0522	-0.0812	0.0318	0.0611	0.1131	0.2943	0.5086	0.5318
	500	-0.0458	-0.0375	-0.0408	0.0217	0.0524	0.0783	0.2427	0.4922	0.4525
	1000	-0.0306	-0.0144	-0.0108	0.0126	0.0368	0.0453	0.1796	0.3964	0.3506

Table 4: The simulation results in $\lambda = 0.6$, $p_1 = 0.3$ and $p_2 = 0.2$

Estimator	n	Bias			MSE			MRE		
		$\hat{\lambda}$	\hat{p}_1	\hat{p}_2	$\hat{\lambda}$	\hat{p}_1	\hat{p}_2	$\hat{\lambda}$	\hat{p}_1	\hat{p}_2
MLE	50	0.1098	0.0340	0.1071	0.0647	0.0243	0.0620	0.3208	0.4098	0.9359
	100	0.0404	0.0038	0.0484	0.0336	0.0189	0.0336	0.2377	0.3827	0.7089
	200	0.0110	-0.0011	0.0050	0.0230	0.0148	0.0196	0.1972	0.3287	0.5569
	500	-0.0041	-0.0047	-0.0141	0.0127	0.0105	0.0118	0.1456	0.2716	0.4443
	1000	-0.002	-0.003	-0.0031	0.0055	0.0048	0.0059	0.0969	0.1821	0.3132
LSE	50	0.0450	0.0323	-0.0771	0.1165	0.0581	0.2139	0.4481	0.5733	1.9004
	100	0.0176	0.0093	-0.0602	0.0754	0.0418	0.1257	0.3591	0.5382	1.4345
	200	0.0181	0.0217	-0.0820	0.0563	0.0329	0.0616	0.3121	0.4902	0.9838
	500	-0.0053	0.0045	-0.0669	0.0329	0.0202	0.0265	0.2477	0.4000	0.6508
	1000	-0.0056	-0.0002	-0.0317	0.0170	0.0115	0.0085	0.1782	0.2995	0.3765
WLSE	50	-0.0417	-0.0475	-0.0075	0.0778	0.0334	0.1620	0.3782	0.4911	1.6246
	100	-0.0368	-0.0364	-0.0245	0.0547	0.0315	0.0814	0.3099	0.4875	1.1433
	200	-0.0115	-0.0088	-0.0330	0.0368	0.0234	0.0350	0.2504	0.4218	0.7422
	500	-0.0108	-0.0066	-0.0264	0.0177	0.0138	0.0158	0.1789	0.3226	0.5017
	1000	-0.0055	-0.0037	-0.0111	0.0086	0.0072	0.0069	0.1247	0.2316	0.3354
ADE	50	0.0199	-0.0215	0.0617	0.0668	0.0336	0.1216	0.3382	0.5014	1.3324
	100	-0.0255	-0.0381	0.0105	0.0446	0.0277	0.0690	0.2805	0.4684	1.0297
	200	-0.0107	-0.0111	-0.0220	0.0315	0.0208	0.0322	0.2327	0.3994	0.7100
	500	-0.0127	-0.0097	-0.0219	0.0168	0.0133	0.0154	0.1743	0.3163	0.4963
	1000	-0.0073	-0.0058	-0.0092	0.0084	0.0071	0.0068	0.1232	0.2291	0.3322
CvME	50	0.1134	0.0235	0.0759	0.1145	0.0584	0.1729	0.4288	0.5783	1.6924
	100	0.0484	0.0056	0.0037	0.0752	0.0419	0.1150	0.3527	0.5370	1.3690
	200	0.0341	0.0196	-0.0457	0.0545	0.0327	0.0539	0.3031	0.4873	0.9240
	500	0.0001	0.0040	-0.0558	0.0324	0.0200	0.0255	0.2448	0.3977	0.6344
	1000	-0.0031	-0.0007	-0.0263	0.0167	0.0114	0.0083	0.1768	0.2984	0.3709
MPSE	50	-0.1164	-0.0455	-0.1610	0.0717	0.0262	0.1832	0.3758	0.4530	1.4599
	100	-0.1280	-0.0761	-0.1132	0.0568	0.0242	0.0721	0.3315	0.4483	1.0265
	200	-0.0950	-0.0621	-0.0648	0.0390	0.0210	0.0301	0.2645	0.3989	0.6808
	500	-0.0566	-0.0381	-0.0366	0.0204	0.0141	0.0130	0.1822	0.3125	0.4600
	1000	-0.0307	-0.0239	-0.0044	0.0080	0.0066	0.0058	0.1141	0.2072	0.3068
TADE	50	-0.0268	-0.0413	0.0233	0.0561	0.0322	0.1066	0.3207	0.5061	1.2465
	100	-0.0371	-0.0410	-0.0052	0.0437	0.0255	0.0580	0.2795	0.4538	0.9305
	200	-0.0365	-0.0288	-0.0277	0.0307	0.0208	0.0289	0.2327	0.3978	0.6663
	500	-0.0222	-0.0155	-0.0264	0.0168	0.0128	0.0138	0.1710	0.3060	0.4767
	1000	-0.0092	-0.0073	-0.0076	0.0071	0.0059	0.0060	0.1096	0.2016	0.3150
MSADE	50	-0.0404	-0.0025	-0.0760	0.0492	0.0323	0.1075	0.2982	0.4616	1.3072
	100	-0.0581	-0.0343	-0.0401	0.0363	0.0238	0.0646	0.2583	0.4217	1.0053
	200	-0.0472	-0.0317	-0.0329	0.0294	0.0209	0.0392	0.2309	0.3936	0.7724
	500	-0.0280	-0.0176	-0.0304	0.0178	0.0151	0.0210	0.1768	0.3252	0.5727
	1000	-0.0228	-0.0180	-0.0058	0.0092	0.0077	0.0085	0.1242	0.2281	0.3698
MSALDE	50	-0.0728	-0.0224	-0.1349	0.0697	0.0365	0.1467	0.3672	0.5174	1.5429
	100	-0.0970	-0.0635	-0.0812	0.0527	0.0297	0.0821	0.3152	0.4940	1.1565
	200	-0.0830	-0.0532	-0.0657	0.0405	0.0267	0.0460	0.2741	0.4610	0.8558
	500	-0.0452	-0.0293	-0.0405	0.0217	0.0164	0.0197	0.1897	0.3427	0.5615
	1000	-0.0351	-0.0273	-0.0059	0.0106	0.0086	0.0076	0.1310	0.2368	0.3474

Table 5: The simulation results in $\lambda = 2$, $p_1 = 0.2$ and $p_2 = 0.4$

Estimator	n	Bias			MSE			MRE		
		$\hat{\lambda}$	\hat{p}_1	\hat{p}_2	$\hat{\lambda}$	\hat{p}_1	\hat{p}_2	$\hat{\lambda}$	\hat{p}_1	\hat{p}_2
MLE	50	0.3739	0.0849	-0.0092	0.5916	0.0279	0.0682	0.3066	0.6328	0.5579
	100	0.2538	0.0714	-0.0598	0.4427	0.0252	0.0500	0.2684	0.6194	0.4746
	200	0.1603	0.0513	-0.0706	0.3391	0.0208	0.0411	0.2320	0.5703	0.4262
	500	0.0809	0.0334	-0.0654	0.2728	0.0161	0.0232	0.2089	0.5053	0.3044
	1000	0.0679	0.0252	-0.0429	0.1440	0.0087	0.0100	0.1505	0.3669	0.1982
LSE	50	0.2185	0.0803	-0.1574	1.2412	0.0623	0.2830	0.4263	0.8045	1.0584
	100	0.2043	0.0645	-0.1153	0.8197	0.0427	0.1469	0.3518	0.6961	0.7636
	200	0.1600	0.0601	-0.1365	0.6762	0.0374	0.1150	0.3227	0.6945	0.6657
	500	0.1341	0.0528	-0.1197	0.5249	0.0280	0.0757	0.2809	0.6138	0.5034
	1000	0.1445	0.0403	-0.0562	0.2723	0.0165	0.0196	0.2026	0.4824	0.2789
WLSE	50	-0.0138	0.0300	-0.1280	0.8810	0.0328	0.2221	0.3707	0.5816	0.9652
	100	0.0819	0.0433	-0.1097	0.6464	0.0287	0.1197	0.3169	0.5999	0.7078
	200	0.1006	0.0437	-0.1027	0.4807	0.0264	0.0748	0.2750	0.6152	0.5624
	500	0.0703	0.0317	-0.0769	0.3521	0.0208	0.0369	0.2307	0.5480	0.3764
	1000	0.0635	0.0237	-0.0463	0.1817	0.0113	0.0144	0.1679	0.4178	0.2374
ADE	50	0.1077	0.0339	-0.0496	0.6554	0.0285	0.1483	0.3175	0.5847	0.7773
	100	0.0713	0.0341	-0.0851	0.5225	0.0246	0.1048	0.2895	0.5810	0.6553
	200	0.0968	0.0399	-0.0906	0.4217	0.0239	0.0688	0.2586	0.5962	0.5375
	500	0.0513	0.0277	-0.0775	0.3405	0.0198	0.0379	0.2275	0.5422	0.3764
	1000	0.0609	0.0225	-0.0443	0.1739	0.0108	0.0139	0.1641	0.4090	0.2321
CvME	50	0.3957	0.0633	-0.0264	1.3051	0.0589	0.2246	0.4308	0.8068	0.9437
	100	0.3181	0.0632	-0.0553	0.8453	0.0419	0.1288	0.3550	0.7006	0.7086
	200	0.2017	0.0544	-0.0999	0.6622	0.0366	0.0971	0.3196	0.6887	0.6241
	500	0.1525	0.0526	-0.1113	0.5289	0.0276	0.0755	0.2821	0.6089	0.4974
	1000	0.1658	0.0424	-0.0500	0.2705	0.0164	0.0185	0.2018	0.4788	0.2714
MPSE	50	-0.5210	0.0142	-0.4051	0.8229	0.0165	0.4023	0.3785	0.4820	1.2314
	100	-0.3548	0.0002	-0.2645	0.6410	0.0176	0.1715	0.3365	0.5406	0.8481
	200	-0.2902	-0.0137	-0.1899	0.5168	0.0177	0.0965	0.2952	0.5660	0.6305
	500	-0.2358	-0.0209	-0.1266	0.4067	0.0165	0.0463	0.2605	0.5411	0.4237
	1000	-0.1580	-0.0177	-0.0719	0.2383	0.0108	0.0173	0.1945	0.4311	0.2520
TADE	50	-0.0654	0.0141	-0.0991	0.5646	0.0218	0.1713	0.3021	0.5547	0.8243
	100	-0.0328	0.0229	-0.1151	0.4629	0.0228	0.1014	0.2770	0.5810	0.6521
	200	-0.0241	0.0177	-0.1016	0.3794	0.0209	0.0673	0.2444	0.5799	0.5269
	500	-0.0286	0.0132	-0.0847	0.3148	0.0174	0.0365	0.2252	0.5375	0.3689
	1000	3×10^{-5}	0.0132	-0.0581	0.1892	0.0106	0.0144	0.1730	0.4183	0.2358
MSADE	50	-0.1474	0.0307	-0.1295	0.1748	0.0186	0.1480	0.1364	0.4697	0.7401
	100	-0.0891	0.0192	-0.0855	0.1405	0.0167	0.0938	0.1187	0.4569	0.6069
	200	-0.0839	0.0071	-0.0732	0.1464	0.0135	0.0583	0.1220	0.4203	0.4879
	500	-0.0588	0.0028	-0.0533	0.1317	0.0099	0.0287	0.1234	0.3744	0.3417
	1000	-0.0378	0.0025	-0.0368	0.0919	0.0067	0.0135	0.1036	0.3079	0.2315
MSALDE	50	-0.3717	0.0242	-0.3079	0.6407	0.0240	0.2884	0.3251	0.5221	1.0745
	100	-0.2395	0.0164	-0.2321	0.5815	0.0264	0.1710	0.3151	0.6082	0.8341
	200	-0.2253	-0.0055	-0.1653	0.4640	0.0202	0.0973	0.2749	0.5792	0.6325
	500	-0.1577	-0.0068	-0.1130	0.3512	0.0172	0.0455	0.2402	0.5417	0.4201
	1000	-0.1008	-0.0073	-0.0602	0.1893	0.0102	0.0163	0.1736	0.4106	0.2515

- The findings of Table 2 ($\lambda = 1.5$, $p_1 = 0.5$, $p_2 = 0.3$) show that all estimators improve systematically as the sample size increases, with decreases observed in bias, MSE, and MRE. The MLE provides satisfactory performance overall and becomes highly efficient for large samples; however, several robust estimators provide competitive or superior accuracy, particularly in smaller sample sizes. Among these, the MSADe estimator shines

by maintaining consistently low bias and stable MSE values across all parameters. The ADE, WLSE, and TADE estimators also show balanced and reliable performance, outperforming LSE in small-sample settings. On the other hand, the LSE and MSALDE produce higher bias and larger MRE, reflecting weaker finite-sample behavior, while MPSE performs moderately but remains inferior to MSADE and ADE. Overall, although the MLE becomes highly efficient as n increases, the robust MSADE presents more stable and accurate estimates for small and medium sample sizes.

- Table 3 provides the simulation results under the setting $\lambda = 0.5$, $p_1 = 0.4$, and $p_2 = 0.5$, demonstrate that all estimators improve steadily with increasing sample size, as reflected by consistent decreases in bias, MSE, and MRE. Among the competing techniques, the MSADE presents the most favorable performance, achieving relatively small bias and the lowest MSE and MRE values across all parameters, particularly for medium and large samples. The ADE, WLSE, and TADE also exhibit stable and reliable estimates, often outperforming the MLE in small sample sizes. Although the MLE becomes increasingly competitive as the sample size increases, it provides higher bias and MSE for small samples. Conversely, the LSE, MPSE, and MSALDE show weaker finite-sample behavior, characterized by larger bias and substantially higher MSE and MRE values, especially for the estimation of p_2 .
- In Table 4, the simulation results based on $\lambda = 0.6$, $p_1 = 0.3$, and $p_2 = 0.2$ are given. The results indicate that all estimators exhibit improved performance as the sample size increases, with notable decreases in bias, MSE, and MRE. Among the competing methods, the MSADE exhibits consistently favorable results, yielding comparatively low bias and stable MSE values across all parameters, particularly for medium and large sample sizes. The ADE, WLSE, and TADE also provide reliable behavior, often surpassing the MLE in small sample sizes. Although the MLE becomes increasingly accurate as n increases, it demonstrates relatively higher bias and MSE levels for small samples, especially in estimating p_2 . On the other hand, the LSE, MPSE, and MSALDE tend to suffer from larger bias and elevated MSE and MRE values, indicating weaker finite-sample performance. Overall, the findings emphasize the robustness and efficiency of the MSADE estimator under this parameter setting.
- Table 5 demonstrates the simulation results under the setting $\lambda = 2$, $p_1 = 0.2$, $p_2 = 0.4$, show that all estimators improve as the sample size increases, as evidenced by decreasing bias, MSE, and MRE values. Among the examined methods, the MSADE provides the best overall performance, achieving consistently lower bias and MSE across all parameters and sample sizes, which indicates strong robustness and efficiency. The ADE and WLSE also perform reliably, frequently outperforming the classical MLE, particularly in smaller samples. Although the MLE becomes competitive as the sample size increases, it presents relatively higher bias and MSE in small sample sizes. On the other hand, the MPSE and MSALDE demonstrate poor finite-sample behavior, characterized by large biases and comparatively high MSE and MRE values. In general, the findings highlight MSADE as the most effective estimator under the simulation scenario.
- The simulation results across all considered settings consistently indicate that the performance of all estimators improves as the sample size increases, with decreases in bias, MSE, and MRE. Among the estimators, the MSADE method emerges as the most robust and efficient, providing consistently low bias and stable MSE values across all

parameters, particularly in medium and large sample sizes. The ADE, WLSE, and TADE also provide reliable and balanced performance, often surpassing the MLE in small sample sizes. The MLE itself becomes highly efficient for large samples, but it tends to show higher bias and MRE in smaller samples, especially for parameters like p_2 . In contrast, the LSE, MPSE, and MSALDE generally show weaker finite-sample behavior, with larger bias and higher MSE and MRE values. In general, for practitioners seeking robust estimation in small to medium samples, we recommend the MSADE for all parameters, while ADE, WLSE, and TADE provide viable alternatives. For very large samples, MLE achieves competitive efficiency and can be reliably used.

6. REAL DATA ANALYSIS

To demonstrate the utility of the CLRBTE distribution, we present three real-world data examples in this section. We also compare the fits to those of some of its competitors, including the exponential, transmuted exponential (TE) (Aryal and Tsokos, 2011), and transmuted generalized Rayleigh (TGR) (Merovci, 2014) distributions. As a result, we take into account the following seven distinct selection criteria: Cramér-von-Mises statistics (CvM), Anderson-Darling statistics (AD), Kolmogorov-Smirnov statistics (KS), Akaike's information criterion (AIC), and associated p-values. The PDFs of fitted models to data sets are shown in Table 6.

Table 6: The list of fitted PDFs to real-world datasets

Distribution	PDF	Range of Parameters
E	$f_E(x; \lambda) = \lambda e^{-\lambda x}$	$\lambda > 0$
TE	$f_{TE}(x; \lambda, \theta) = (1 + \theta)\lambda e^{-\lambda x} - 2\theta(1 - e^{-\lambda x})\lambda e^{-\lambda x}$	$\lambda > 0, -1 < \theta < 1$
TGR	$f_{TGR}(x; \lambda, \beta, \theta) = 2\lambda\beta^2 x e^{-(\beta x)^2} (1 - e^{-(\beta x)^2})^{\lambda-1} \left[1 + \theta - 2\theta (1 - e^{-(\beta x)^2})^\lambda \right]$	$\lambda, \beta > 0, -1 < \theta < 1$

6.1. Survival time data

In this subsection, we analyze a well-known right-skewed sample of survival times (in days) for patients diagnosed with acute myelogenous leukemia, originally reported in Feigl and Zelen (1965). The survival time dataset is as follows: 65, 156, 100, 134, 16, 108, 121, 4, 39, 143, 56, 26, 22, 1, 1, 5, 65, 56, 65, 17, 7, 16, 22, 3, 4, 2, 3, 8, 4, 3, 30, 4, 43. Table 8 shows the MLEs and corresponding standard errors (SEs) of the parameters for the fitted models while Table 7 provides the selection criteria for the survival time data. The fitted CDF and PDF plots are shown in Figures 4 and 5 respectively.

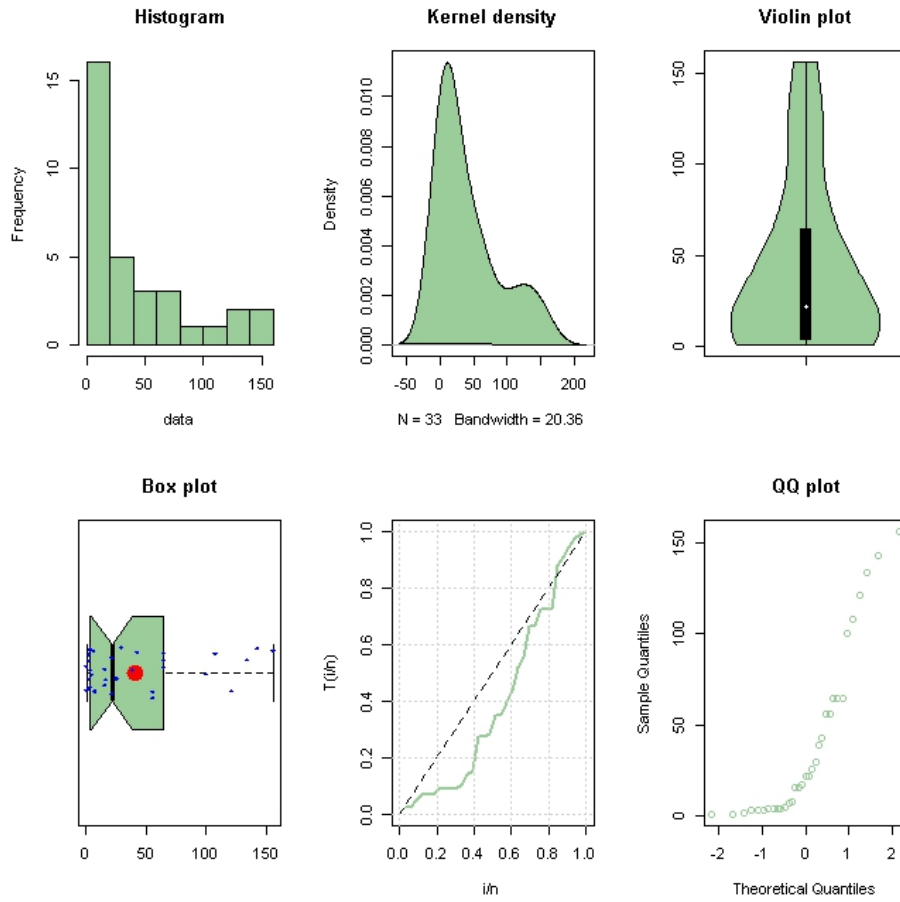


Figure 3: Non-parametric plots for survival time data

Figure 3 illustrates a variety of non-parametric graphical methods utilized for survival time data. The data distribution exhibits significant skewness, with most observations concentrated at lower levels. The kernel density and violin plots demonstrate multimodality, signifying various substructures within the data. The Q-Q plot significantly deviates from the reference line, indicating a deficiency in normality, however the box plot corroborates the presence of outliers.

Table 7: The comparison statistics for the survival time data

Distribution	AIC	KS	AD	CvM	p-value(KS)	p-value(AD)	p-value(CvM)
CLRBTE	312.4142	0.1044	0.4992	0.0643	0.8646	0.7464	0.7901
TE	313.7042	0.2028	1.7879	0.2542	0.1325	0.1208	0.1832
E	312.9003	0.2182	2.3066	0.3250	0.0863	0.0631	0.1148
TGR	312.8599	0.1318	0.6735	0.1003	0.6156	0.5801	0.5862

Table 8: The MLEs and SEs of the parameters for the survival time data

Distribution	$\hat{\lambda}$	\hat{p}_1	\hat{p}_2	$\hat{\theta}$	$\hat{\beta}$	SE($\hat{\lambda}$)	SE(\hat{p}_1)	SE(\hat{p}_2)	SE($\hat{\theta}$)	SE($\hat{\beta}$)
CLRBTE	0.0174	0.6369	0.0878	-	-	0.0055	0.3458	0.6688	-	-
TE	0.0206	-	-	0.3704	-	0.0057	-	-	0.3617	-
E	0.0245	-	-	-	-	0.0043	-	-	-	-
TGR	0.3066	-	-	0.4216	0.0089	0.0608	-	-	0.4719	0.0025

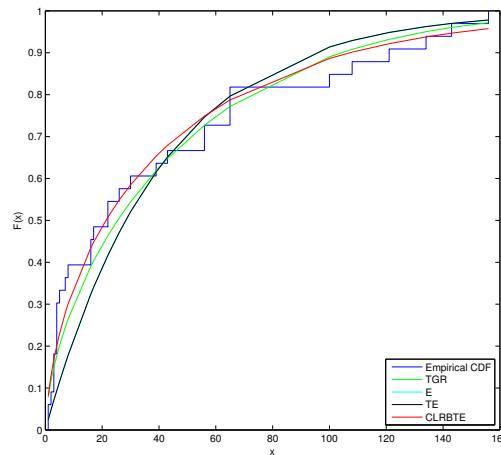


Figure 4: The fitted CDFs for the survival time data

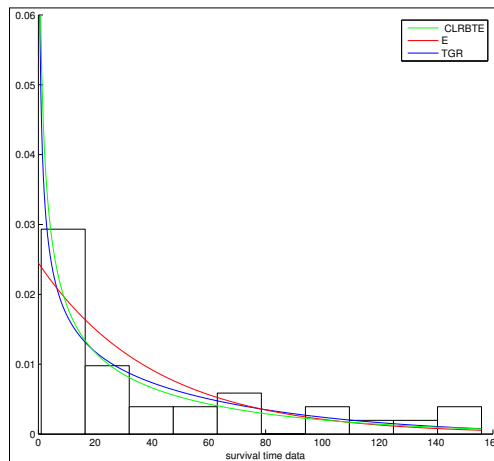


Figure 5: The fitted PDFs for the survival time data

Based on all of the selection criteria listed in Table 7, we identify the CLRBTE distribution as the model that fits the survival time dataset the best out of all the models. It is evident from Figures 4 and 5 that the closest model to the survival time dataset is the CLRBTE distribution.

6.2. Failure time data

In this subsection, we analyze the data set provided by Murthy et al. (2004), denotes the failure times of 20 components. The failure time data are: 0.0003, 0.0298, 0.1648, 0.3529, 0.4044, 0.5712, 0.5808, 0.7607, 0.8188, 1.1296, 1.2228, 1.2773, 1.9115, 2.2333, 2.3791, 3.0916, 3.4999, 3.7744, 7.4339, 13.6866. Table 9 provides the selection criteria while Table 10 gives the MLEs and their SEs for the failure time data. Furthermore, the fitted CDF and PDF plots are shown in Figures 7 and 8 respectively.

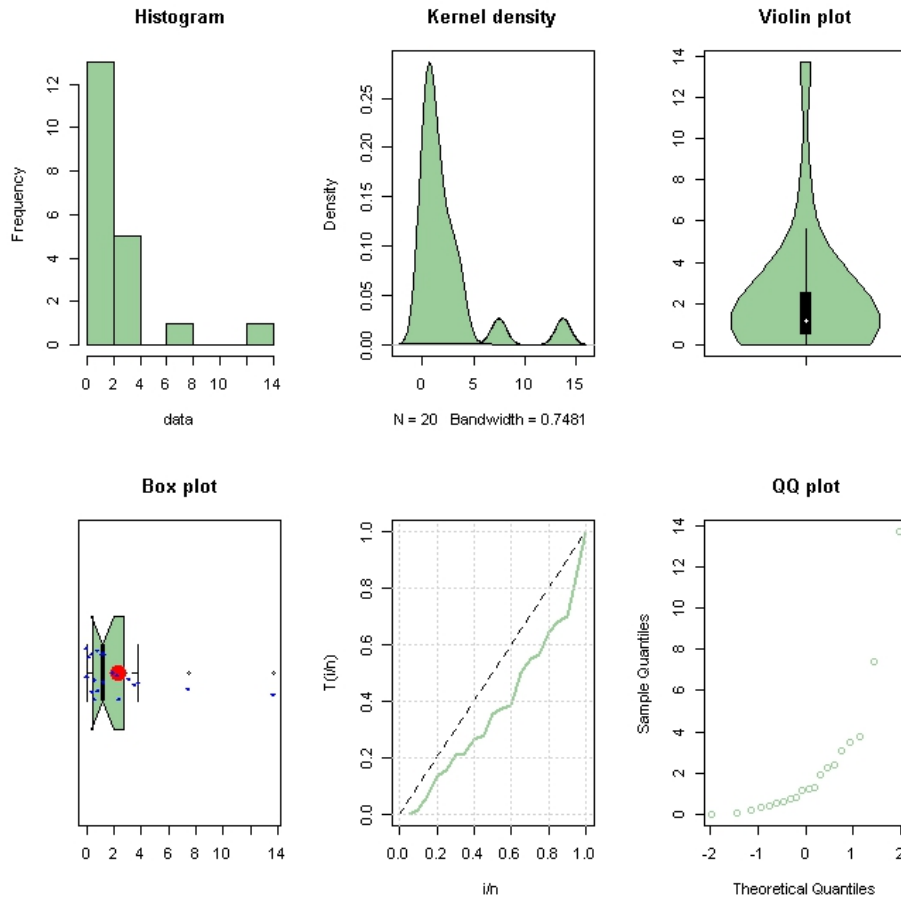


Figure 6: Non-parametric plots for failure time data

Failure time data nonparametric summaries are shown in Figure 6. From Figure 6, the failure dataset displays a heavy right skew. The density estimate indicates a dominant peak alongside secondary fluctuations, consistent with the characteristics of the potential mixture.

Table 9: The comparison statistics for the failure time data

Distribution	AIC	KS	AD	CvM	p-value(KS)	p-value(AD)	p-value(CvM)
CLRBTE	74.2783	0.1126	0.3306	0.0345	0.9371	0.9126	0.9627
TE	75.1337	0.1241	0.6187	0.0463	0.8810	0.6283	0.9032
E	74.7239	0.1691	0.9941	0.1104	0.5597	0.3593	0.5401
TGR	73.6468	0.1274	0.3710	0.0545	0.8619	0.8756	0.8540

Table 10: The MLEs and SEs of the parameters for the failure time data

Distribution	$\hat{\lambda}$	\hat{p}_1	\hat{p}_2	$\hat{\theta}$	$\hat{\beta}$	SE($\hat{\lambda}$)	SE(\hat{p}_1)	SE(\hat{p}_2)	SE($\hat{\theta}$)	SE($\hat{\beta}$)
CLRBTE	0.2098	0.2510	0.5475	-	-	0.2231	0.6935	0.6300	-	-
TE	0.3213	-	-	0.6236	-	0.1115	-	-	0.4071	-
E	0.4413	-	-	-	-	0.0987	-	-	-	-
TGR	0.2717	-	-	0.7501	0.1099	0.0578	-	-	0.4221	0.0483

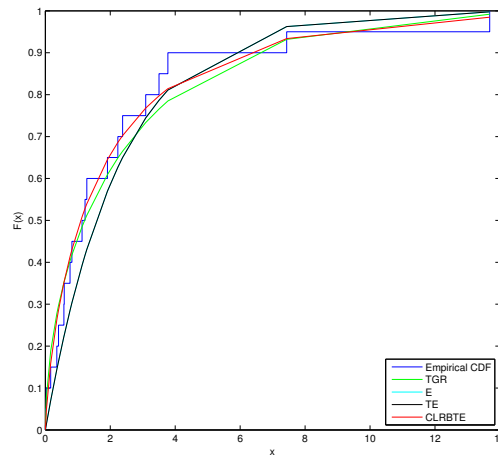


Figure 7: The fitted CDFs for the failure time data

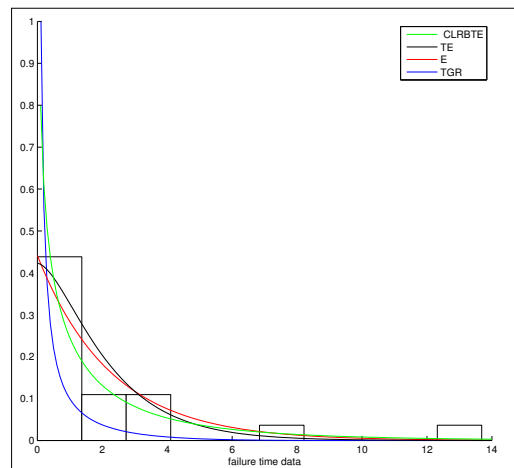


Figure 8: The fitted PDFs for the failure time data

From Figures 7 and 8, we observe that the best-fitted model is CLRBTE distribution for the failure dataset.

7. CONCLUSION

Through the present study, we introduce a new family of distributions based the distributions of the first three lower record values to the literature. We also examine in detail a special case of the proposed family based on the exponential distribution. We present some statistical properties of the CLRBTE distribution, including point estimation, a simulation study, and its application to real-life data. Nine different estimators have been proposed for point estimation. A MC simulation study has been designed to compare the performance of these estimators based on bias, MSE, and MRE across four different parameter settings, varying sample sizes, and a 5000-iteration. As a result of the simulation study, it has been

concluded that MSADE is a good alternative to MLE in estimating the parameters of the CLRBTE distribution. Subsequently, the CLRBTE distribution fit both datasets better than potential competitors E, TE, and TGR, according to seven different comparison criteria in the two real data analyses. In future studies, new members can be proposed for the suggested family of distributions.

ACKNOWLEDGMENTS

The author thanks anonymous reviewers for their valuable comments and the handling editor for their guidance throughout the review process.

REFERENCES

- Ahmad, A., Ahmad, S., and Ahmed, A. (2014). Transmuted inverse rayleigh distribution: A generalization of the inverse rayleigh distribution. *Mathematical Theory and Modeling*, 4(7):90–98.
- Alrweili, H. (2025). Statistical inference and data analysis of the record-based transmuted burr x model. *Open Mathematics*, 23(1):20240121.
- Arnold, B. C., Balakrishnan, N., and Nagaraja, H. N. (2008). *A First Course in Order Statistics*. SIAM.
- Arshad, M., Khetan, M., Kumar, V., and Pathak, A. K. (2024). Record-based transmuted generalized linear exponential distribution with increasing, decreasing and bathtub shaped failure rates. *Communications in Statistics-Simulation and Computation*, 53(7):3489–3513.
- Aryal, G. R. and Tsokos, C. P. (2011). Transmuted weibull distribution: A generalization of the weibull probability distribution. *European Journal of Pure and Applied Mathematics*, 4(2):89–102.
- Azhad, Q. J., Arshad, M., Devi, B., Khandelwal, N., and Ali, I. (2023). Record-based transmuted kumaraswamy generalized family of distributions: properties and application. In *G Families of Probability Distributions*, pages 233–243. CRC Press.
- Balakrishnan, N. and He, M. (2021). A record-based transmuted family of distributions. *Advances in Statistics-Theory and Applications: Honoring the Contributions of Barry C. Arnold in Statistical Science*, pages 3–24.
- Cheng, R. and Amin, N. (1983). Estimating parameters in continuous univariate distributions with a shifted origin. *Journal of the Royal Statistical Society: Series B (Methodological)*, 45(3):394–403.
- Choi, K. and Bulgren, W. G. (1968). An estimation procedure for mixtures of distributions. *Journal of the Royal Statistical Society: Series B (Methodological)*, 30(3):444–460.
- Feigl, P. and Zelen, M. (1965). Estimation of exponential survival probabilities with concomitant information. *Biometrics*, pages 826–838.
- Granzotto, D., Louzada, F., and Balakrishnan, N. (2017). Cubic rank transmuted distributions: inferential issues and applications. *Journal of Statistical Computation and Simulation*, 87(14):2760–2778.
- Mahmoud, M. and Mandouh, R. (2013). On the transmuted fréchet distribution. *Journal of Applied Sciences Research*, 9(10):5553–5561.

- Merovci, F. (2014). Transmuted generalized rayleigh distribution. *Journal of Statistics Applications & Probability*, 3(1):9.
- Murthy, D. P., Xie, M., and Jiang, R. (2004). *Weibull models*. John Wiley & Sons.
- Nocedal, J. and Wright, S. (2006). *Numerical Optimization*. Springer Science & Business Media, New York, 2 edition.
- Pathak, A. K., Arshad, M., Pandey, A. K., and Ali, A. (2024). Record-based transmuted unit-omega distribution: different methods of estimation and applications: Accepted-august 2024. *REVSTAT-Statistical Journal*.
- R Core Team (2024). *R: A Language and Environment for Statistical Computing*. R Foundation for Statistical Computing, Vienna, Austria.
- Ranneby, B. (1984). The maximum spacing method. an estimation method related to the maximum likelihood method. *Scandinavian Journal of Statistics*, pages 93–112.
- Sakthivel, K. and Nandhini, V. (2022). Record-based transmuted power lomax distribution: properties and its applications in reliability. *Reliability: Theory & Applications*, 17(4 (71)):574–592.
- Saraçoğlu, B. and Taş, C. (2018). A new statistical distribution: cubic rank transmuted kumaraswamy distribution and its properties. *Journal of the National Science Foundation of Sri Lanka*, 46(4).
- Shaw, W. and Buckley, I. (2009). The alchemy of probability distributions: beyond gram-charlier expansions, and a skew-kurtotic-normal distribution from a rank transmutation map. *arXiv preprint arXiv:0901.0434*.
- Swain, J. J., Venkatraman, S., and Wilson, J. R. (1988). Least-squares estimation of distribution functions in johnson’s translation system. *Journal of Statistical Computation and Simulation*, 29(4):271–297.
- Taş, C. (2021). Transmuted lower record type power function distribution. *Journal of Science and Arts*, 21(4):951–960.
- Taş, C. (2022). Transmuted lower record type inverse rayleigh distribution: estimation, characterizations and applications. *Ricerche di Matematica*, 71(2):777–802.
- Taş, C. (2024). A new lindley distribution: applications to covid-19 patients data. *Soft Computing*, 28(4):2863–2874.
- Taş, C. (2025a). Record-based transmuted exponential power distribution: theory, simulation, and applications. *The Journal of Supercomputing*, 82(1):39.
- Taş, C. (2025b). Record-based transmuted log-logistic distribution: Properties, simulation, and applications to petroleum rock and reactor pump data: Accepted november 2025. *REVSTAT-Statistical Journal*.
- Taş, C. (2026). Cubic ranked record based transmuted family of distributions: Applications and properties. *Communications in Statistics-Theory and Methods*, 55(6):1933–1953.
- Taş, C. and Saraçoğlu, B. (2022a). Cubic rank transmuted inverse rayleigh distribution: Properties and applications. *Sigma Journal of Engineering and Natural Sciences*, 40(2):421–432.
- Taş, C. and Saraçoğlu, B. (2022b). On the record-based transmuted model of balakrishnan and he based on weibull distribution. *Communications in Statistics-Simulation and Computation*, 51(8):4204–4224.
- Taş, C. and Saraçoğlu, B. (2023). Cubic rank transmuted generalized gompertz distribution: properties and applications. *Journal of Applied Statistics*, 50(1):195–213.

- Tamış, C., Saraçoğlu, B., Kuş, C., and Pekgör, A. (2020). Transmuted complementary exponential power distribution: properties and applications. *Cumhuriyet Science Journal*, 41(2):419–432.
- Tamış, C., Saraçoğlu, B., Kuş, C., Pekgör, A., and Karakaya, K. (2021). Transmuted lower record type fréchet distribution with lifetime regression analysis based on type i-censored data. *Journal of Statistical Theory and Applications*, 20(1):86–96.
- Torabi, H. (2008). A general method for estimating and hypotheses testing using spacings. *Journal of Statistical Theory and Applications*, 8(2):163–168.